ELSEVIER

Journal of Organometallic Chemistry 660 (2002) 153–160

Journal of Organometallic Chemistry

www.elsevier.com/locate/jorganchem

Pyrolysis of $[Ru_3(CO)_{10}(dppe)]$: activation of C–H and P–Ph bonds. The crystal structure and dynamical behavior of $[Ru_4(CO)_9(\mu\text{-}CO)\{\mu_4\text{–}\eta^2\text{-}PCH_2CH_2P(C_6H_5)_2\}(\mu_4\text{–}\eta^4\text{-}C_6H_4)]$

Gloria Sánchez-Cabrera, Francisco J. Zuno-Cruz, María J. Rosales-Hoz *, Vladimir I. Bakhmutov

Departamento de Química, Centro de Investigación y de Estudios Avanzados del I.P.N., 2508 Col. San Pedro Zacatenco, Apdo. Postal 14-740, Mexico D.F. 07000, Mexico

Received 15 May 2002; received in revised form 1 August 2002; accepted 4 August 2002

Abstract

The pyrolysis reaction of $[Ru_3(CO)_{10}(dppe)]$, compound **1**, in toluene yields as the main product $[Ru_4(CO)_9(\mu\text{-}CO)\{\mu_4\text{–}\eta^2\text{-}PCH_2CH_2P(C_6H_5)_2\}(\mu_4\text{–}\eta^4\text{-}C_6H_4)]$, compound **2**. The X-ray structure of **2** shows a benzyne group coordinated to a square of ruthenium atoms and a $\mu_4\text{–}\eta^2\text{-}PCH_2CH_2PPh_2$ fragment. Variable-temperature NMR experiments showed three independent dynamic processes: a rotation of the benzyne group, CO migration and a twisting movement of the $CH_2\text{–}CH_2$ fragment. The thermolysis of $[Ru_3(CO)_{10}(dfppe)]$, compound **3**, (dfppe = 1,2-bis(dipentafluorophenylphosphino)ethane, carried out under the same conditions, showed **3** to be stable.

Keywords: Tetraruthenium cluster; Benzyne; Dynamic process

1. Introduction

Pyrolysis of carbonyl cluster compounds, both in solution and in the solid state, have produced a wide range of reactions which involve activation of different types of bonds. Pyrolysis of $[Os_3(CO)_{12}]$ leads to higher nuclearity clusters and, under some conditions, disproportionation of the cluster producing carbon atoms which become an integral part of the cluster as carbide groups [1]. Substituted phosphine and phosphite clusters have been reported to suffer activation of several O–C bonds [2] and C–H and P–C bonds [3].

Solution pyrolysis of $[Ru_3(CO)_{11}(PPh_3)]$ in toluene produced tetranuclear and pentanuclear clusters containing benzyne groups, products from the rupture of P–Ph bonds, as well as μ_4-PPh groups [4]. On the other hand, pyrolysis of the arsine analog, $[Ru_3(CO)_{11}(AsPh_3)]$, resulted in mainly $[Ru_2(CO)_6(\mu\text{-}AsPh_2)_2]$. Reactivity of clusters containing polydentate phosphine groups are less known. To our knowledge, only the pyrolysis of $[Ru_3(\mu\text{-dppm})(CO)_{10}]$ and of $[Ru_3(CO)_9(\mu\text{-dppm})(PPh_3)]$ has been described [5,6], where oxidative addition of P–C and C–H aromatic bonds of the dppm ligand occurs together with cluster disproportionation.

Our interest in determining the effects of fluorine substituted ligands in transition metal clusters, led us recently to prepare [7] $[Ru_3(CO)_{10}(dfppe)]$, (**3**), (dfppe = 1,2-bis(dipentafluorophenylphosphino)ethane). A comparison of the reactivity of $[Ru_3(CO)_{10}(dppe)]$ and **3** under thermal conditions motivated us to carry out the pyrolysis reaction of both compounds. The study could also help us to rationalize the results of the synthesis of both derivatives through thermal activation. Results are described herein.

The main product of the pyrolysis of $[Ru_3(CO)_{10}(dppe)]$, has a benzyne group coordinated to a tetraruthenium fragment. This compound shows a benzyne 'rotation' such as the ones reported in $[Ru_3(CO)_7(\mu\text{-}PPh_2)_2(\mu_3\text{–}\eta^2\text{-}C_6H_4)]$, [8] $[Os_3(CO)_7(\mu\text{-}$

* Corresponding author. Tel.: +52-5747-3800; fax: +52-5747-7113
E-mail address: mrosales@mail.cinvestav.mx (M.J. Rosales-Hoz).

0022-328X/02/$ - see front matter
PII: S0022-328X(02)01817-X

$EMe_2)_2(\mu_3-\eta^2-C_6H_4)]$ (E = P [9], As [10]) and $[Ru_4(CO)_{10}(\mu\text{-}CO)(\mu_4\text{-}PPh)(\mu_4-\eta^4-C_6H_4)]$ [4] (compound **4**). On the basis of the fast-migrating CO groups in square tetranuclear metal carbonyls [11], the dynamic behavior of **4** was explained in terms of a merry-go-round mechanism where the benzyne ring undergoes a contra-rotation, kinetically limiting the CO migration. The latter means that rates and energies of both processes should be identical. However, the benzyne rotation in complex **4** is not directly observable in the NMR spectra. Therefore, a merry-go-round mechanism requires evidence. Finally the process observed in **4**, was not characterized quantitatively. In this paper we also report on the NMR behavior of complex **2**. This complex has no symmetry because of the presence of the chelating phosphine and hence it is a good model for independent observations of both dynamic processes.

2. Results and discussion

2.1. Characterization of $[Ru_4(CO)_9(\mu\text{-}CO)\{\mu_4-\eta^2\text{-}PCH_2CH_2P(C_6H_5)_2\}(\mu_4-\eta^4\text{-}C_6H_4)]$ (2)

The main product of the thermolysis of **1**, carried out in refluxing toluene for 2 h, compound **2** (Scheme 1), was separated by silica thin layer chromatography. In the reaction, three other unidentified products were observed; spectroscopic evidence for these compounds showed that their structures could correspond to Ru_5 and Ru_3 clusters. Compound **2** was characterized spectroscopically (Table 1), and showed two doublets in the $^{31}P\{^1H\}$-NMR spectrum, at 398.7 (P_2) and 80.7 ppm (P_1), ($^2J(^{31}P-^{31}P) = 5.4$ Hz). The chemical shift of the P_2 is very similar to the one reported for **4** [4] where the phosphorus atom is bonded to the four metal atoms.

Table 1
^1H-, ^{31}P-, and ^{13}C-NMR data for **2**

^1H [a] δ (ppm)	$^{31}P\{^1H\}$ [b] δ (ppm) [$^2J31_P-31_P$] {$^3J31_P-31_P$}	$^{13}C\{^1H\}$ [c] δ (ppm) [$^nJ13_C-31_P$]
7.46 (m) (Ph), 6.76 (AA′) (CH), 6.03 (XX′) (CH),	398.7 (d) (P_2) 80.7 (d) (P_1)	197.6 (br) (CO) 144.1 (br) (Cc,c′)
$^3J_{1H^1H} = 3.7$ 3.35 (ddt) (CH_2e)	[5.4]	133.9 (d) [$^1J = 49.1$]*i* 131.8 (d) [$^2J = 9.8$]*o*
$^2J_{1He^{31}P_1} = 20.8$		131.1 (s)*p*
$^3J_{1He^{31}P_2} = 7.2$		128.9 (d) [$^3J = 12.3$]*m*
$^3J_{1He^1Hd} = 7.2$		126.6 (s) (Ca,a′)
2.71 (ddt) (CH_2d)		110.3 (br) (Cb,b′),
$^2J_{1Hd^{31}P_2} = 24.1$		32.6 (s) (Ce)
$^3J_{1Hd^{31}P_1} = 9.9$		29.7 (s) (Cd)
$^3J_{1He^1Hd} = 7.2$		

[a] Recorded at 300.130 MHz.
[b] Recorded at 121.519 MHz.
[c] Recorded at 100.535 MHz. $CDCl_3$. J Hz^{-1}. (s) singulete, (d) doublet, (t) triplet, (br) broad, (m) multiplet, *o*, *ortho*; *p*, *para*; *m*, *meta*; *i*, *ipso*.

The room temperature ^1H-NMR spectrum of **2** shows a typical AA′XX′ pattern (δ(A, A′) = 6.76 ppm, δ(X, X′) = 6.03 ppm) suggesting the presence of the benzyne ring, coordinated in a $\mu_4-\eta^4$-fashion. This conclusion is well supported by the room-temperature $^{13}C\{^1H\}$-NMR spectrum exhibiting signals at 144.1, 126.6 and 110.3 ppm (broadened) assigned to the μ-C (C(c)), the CH uncoordinated (C(a)) and coordinated (C(b)) carbons respectively, (see Scheme 1). In addition this spectrum shows a broadened CO resonance at 197.6 ppm and two singlet lines of the CH_2-CH_2 bridge (32.6 and 29.7 ppm). Finally this CH_2-CH_2 bridge appears in the

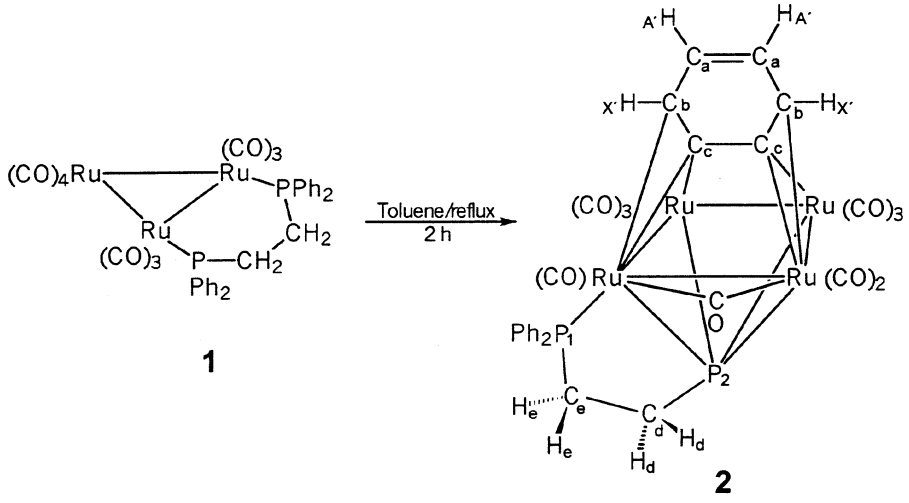

Scheme 1. Reaction scheme for the thermolysis of compound **1**.

room-temperature ^{1}H-NMR spectrum as a well resolved AA′XX′ system at 2.71 and 3.35 ppm. Selective ^{31}P irradiation experiments have revealed that the line at 2.71 ppm, a doublet of doublets of triplets, corresponds to the methylene group bonded directly to the phosphinidene fragment ($^{2}J(H–P_2) = 24.1$, $^{3}J(H–P_1) = 9.9$, $^{3}J(H–H) = 7.2$ Hz) while the resonance at 3.35 ppm is assigned to the CH_2 group bonded to the phosphine end of the ligand ($^{2}J(H–P_2) = 20.8$, $^{3}J(H–H) = 7.3$, $^{3}J(H–P_1) = 7.2$ Hz). All the data demonstrate that complex **2** is fluxional at room temperature: the CO and benzyne migrations are fast on the NMR time scale.

In order to confirm the molecular structure of **2**, an X-ray diffraction study was undertaken. Results are shown in Fig. 1 and Table 2. An analysis demonstrates the structure to be similar to the already described tetranuclear-PPh compound, $[Ru_4(CO)_{10}(\mu\text{-}CO)(\mu_4\text{-}PPh)(\mu_4–\eta^4\text{-}C_6H_4)]$ (**4**). This consists of a square metal plane bridged on one face of the square by a phosphinidene ligand, but in **2** the μ_4-$PCH_2CH_2PPh_2$ group is also bonded through the phosphine ligand to one of the ruthenium atoms. The phosphorus atom P(2) is found at 1.2116(4) Å above the plane formed by the four metal atoms. The benzyne group is located at the other side of the square metal plane. One of the edges (Ru(1)–Ru(4)) of the Ru_4 square is bridged by a carbonyl ligand. Metal–metal bond distances range from 2.819(1) to 2.935(1) Å; the shortest value corresponds to the edge bridged by the carbonyl group, while the longest is

Table 2
Selected bond lengths (Å) and angles (°) for **2**

Bond lengths			
Ru(1)–Ru(3)	2.907(1)	C(50)–C(51)	1.53(1)
Ru(3)–Ru(2)	2.935(1)	Ru(1)–C(7)	2.57(1)
Ru(2)–Ru(4)	2.892(2)	Ru(1)–C(8)	2.303(9)
Ru(4)–Ru(1)	2.819(1)	Ru(3)–C(8)	2.09(1)
Ru(1)–P(1)	2.310(3)	Ru(4)–C(10)	2.63(1)
Ru(1)–P(2)	2.384(3)	Ru(4)–C(9)	2.317(9)
Ru(4)–P(2)	2.428(3)	Ru(2)–C(9)	2.12(1)
Ru(2)–P(2)	2.333(3)	C(7)–C(8)	1.41(2)
Ru(3)–P(2)	2.356(3)	C(8)–C(9)	1.44(1)
Ru(1)–C(4)1	2.01(1)	C(9)–C(10)	1.41(1)
Ru(4)–C(4)1	2.11(2)	C(10)–C(11)	1.41(2)
P(1)–C(50)	1.83(1)	C(11)–C(12)	1.36(2)
P(2)–C(51)	1.83(1)	C(12)–C(7)	1.41(2)
Bond angles			
Ru(4)–Ru(1)–Ru(3)	91.17(4)	Ru(2)–P(2)–Ru(1)	119.6(1)
Ru(4)–Ru(2)–Ru(3)	89.15(4)	Ru(3)–P(2)–Ru(4)	117.5(1)
Ru(1)–Ru(4)–Ru(2)	91.09(4)	P(1)–Ru(1)–C(7)	91.0(4)
Ru(1)–Ru(3)–Ru(2)	88.50(4)	P(1)–Ru(1)–C(8)	151.3(3)
Ru(3)–Ru(1)–P(2)	51.74(7)	C(13)–Ru(1)–C(7)	81.2(4)
Ru(2)–Ru(4)–P(2)	51.11(7)	C(13)–Ru(1)–C(8)	111.5(4)
Ru(1)–Ru(3)–P(2)	52.61(7)	C(41)–Ru(1)–P(2)	98.1(3)
Ru(4)–Ru(2)–P(2)	54.11(7)	C(41)–Ru(4)–P(2)	96.1(3)
Ru(3)–P(2)–Ru(1)	75.65(8)	C(41)–Ru(1)–C(7)	91.0(4)
Ru(1)–P(2)–Ru(4)	71.69(8)	C(41)–Ru(1)–C(8)	99.6(4)
Ru(4)–P(2)–Ru(2)	74.78(8)	C(41)–Ru(1)–P(2)	100.3(3)
Ru(2)–P(2)–Ru(3)	77.50(9)	C(41)–Ru(4)–C(9)	99.6(4)
P(2)–Ru(1)–P(1)	81.9(1)	C(41)–Ru(4)–C(10)	93.4(4)

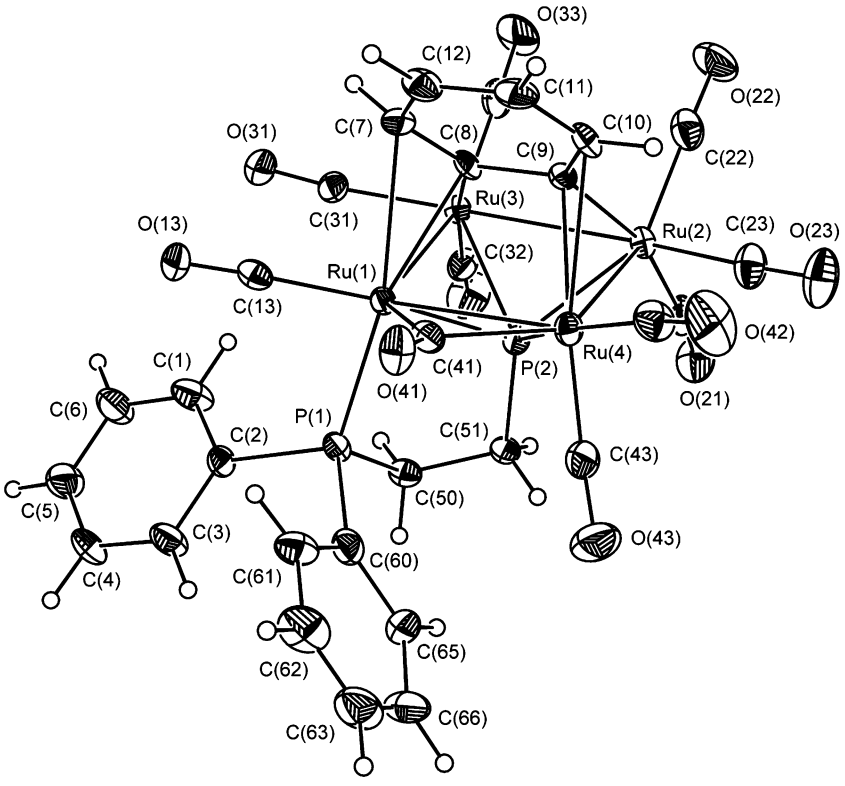

Fig. 1. Structure of Compound **2**, including numbering scheme. ORTEPS shown at 40% probability.

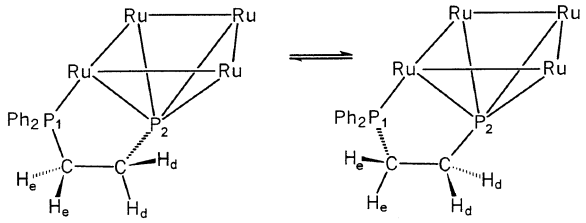

Scheme 2. Twisting movement of the CH_2–CH_2 fragment in compound **2**. The benzyne and CO groups are ommited for clarity.

Ru(2)–Ru(3), where the two metal atoms are σ-bonded to the benzyne ligand. The μ_4-P–Ru bonds are different and the average value is shorter than in **4**. The Ru–P(1) bond length is short with respect to the bonds of the bridging phosphorus group.

The benzyne ligand is coordinated to the four metal atoms through two σ- and two π-bonds. All the C–C– distances are similar to those observed in **4**. The μ_4-benzyne ligand has four equivalent C–C distances, one shorter C(11)–C(12) distance (1.36(2) Å) and one larger C(8)–C(9) distance (1.44(1) Å), where the last value corresponds to the carbons which are bonded to the metal atoms. This is probably due to a localization of the π-electrons of the ring caused by the two η^2-interactions. All the σ- and π-interactions M–C in **2** are found in the same range 2.11(1)–2.12(1), 2.292(4)–2.32(1) and 2.58(1)–2.69(1) Å respectively, as those observed for compounds $[Ru_4(CO)_{10}(\mu\text{-}CO)(\mu_4\text{-}PPh)(\mu_4\text{–}\eta^4\text{-}C_6H_4)]$ (**4**) and $[Ru_4(CO)_{10}(\mu\text{-}CO)(\mu_4\text{-}PCH_2NPh_2)(\mu_4\text{–}\eta^4\text{-}C_6H_4)]$ [4]. The σ-interaction Ru(3)–C(8) and the π-interaction Ru(1)–C(7) are slightly shorter (2.09(1) and 2.57(1) Å, respectively). Finally the benzyne plane forms an angle of 51.4° with the tetranuclear metal plane. This interplanar angle is similar to the value reported for compounds **4** and $[Ru_4(CO)_{10}(\mu\text{-}CO)(\mu_4\text{-}PCH_2NPh_2)(\mu_4\text{–}\eta^4\text{-}C_6H_4)]$, 51.85 average and 50.9°, respectively.

2.2. Variable temperature NMR studies of $[Ru_4(CO)_9(\mu\text{-}CO)\{\mu_4\text{–}\eta^2\text{-}PCH_2CH_2P(C_6H_5)_2\}(\mu_4\text{–}\eta^4\text{-}C_6H_4)]$ (2)

As it was expected, the $^{13}C\{^1H\}$-NMR spectra depend on the temperature. On cooling to 193 K, the broadened CO resonance, observed at room temperature at 197.6 ppm, transforms to five broadened lines with δ of 196.8(s), 197.5 (d, $J(^{13}C\text{–}^{31}P) \approx 33$ Hz) 197.9 (s), 200.5(d, $J(^{13}C\text{–}^{31}P) \approx 33$ Hz and 205.3 ppm (d, $J(^{13}C\text{–}^{31}P) \approx 40$ Hz). The lowest field resonance can be attributed to the bridging CO group [4]. The structure in Fig. 1 shows that all the carbonyl groups are different in complex **2**. Thus by analogy with complex **4** [4], the low-temperature spectrum of **2** corresponds to a situation, when the rotational exchange within the two $Ru(CO)_3$ groups still operates on the NMR time scale. In contrast, the carbon signals of the benzyne ring are observed now as six single lines at 145.90 (C(c′)), 141.5 ppm (C(c)), 128.0 (C(a′)), 125.1 ppm (C(a)), 113.2 (C(b′)) and 104.6 ppm (C(b)). Note that each higher-field resonance in the pair of the magnetically-nonequivalent carbons (C(c) and C(b)) is broadened by 4–5 Hz due to a $^{31}P_1\text{–}^{13}C$ coupling, (see Fig. 2). This effect provided the above assignments. In accord with the ^{13}C-NMR data, the ^1H resonances of the benzyne ring also showed a temperature evolution from an AA′XX′ pattern at 295 K to two triplets (6.77 and 6.66 ppm) and two doublets (6.02 and 5.88 ppm) at 193 K (Fig. 2). Thus at low temperature the fast ring motion in **2** is frozen on the NMR time scale. The full line-shape analysis of the ^{13}C signals of the benzyne ring by the DSYNPC [12] program resulted in the kinetic parameters of the dynamic process; $\Delta H^{\neq} = 11.5 \pm 0.3$ kcal mol^{-1} and $\Delta S^{\neq} = 0.5 \pm 0.5$ eu. It is important that the entropy value (close to zero) corresponds well to the intramolecular character of the process.

Beside the CO and benzyne migrations, the ^1H-NMR spectrum of **2** showed a non-rigidity of the CH_2–CH_2 bridge. Actually the protons in each methylene group are equivalent at room temperature as the result of the former processes. However, on cooling the CH_2 signals are broadened to give finally four lines at 3.49, 3.03, 2.98 and 2.23 ppm. Unfortunately because of the complexity of the exchanging spin system it was possible only to estimate the ΔG^* energy of the process as 9.4 kcal mol^{-1} at coalescence temperature (213 K). The ΔG^* (213 K) value calculated for the benzyne migration, is higher (11.4 kcal mol^{-1}) and hence both motions can be considered as independent ones. It is important that even at 193 K the above four resonances are very broadened (Fig. 3) demonstrating the presence of an additional dynamic process, this could be due to the twisting of the CH_2–CH_2 bridge presented in Scheme 2. Finally the ^{31}P-NMR spectra of **2** have shown no temperature changes.

Cooperative CO/benzyne migrations suggested for symmetrical complex **4** [4], operate with the equivalent states. In addition the ring movement control kinetically the CO migrations in such a merry-go-round mechanism. The same scheme, applied for complex **2**, leads to appearance of structurally-nonequivalent states. However, the low-temperature NMR data demonstrate the presence of one state only. It is reasonable that this state

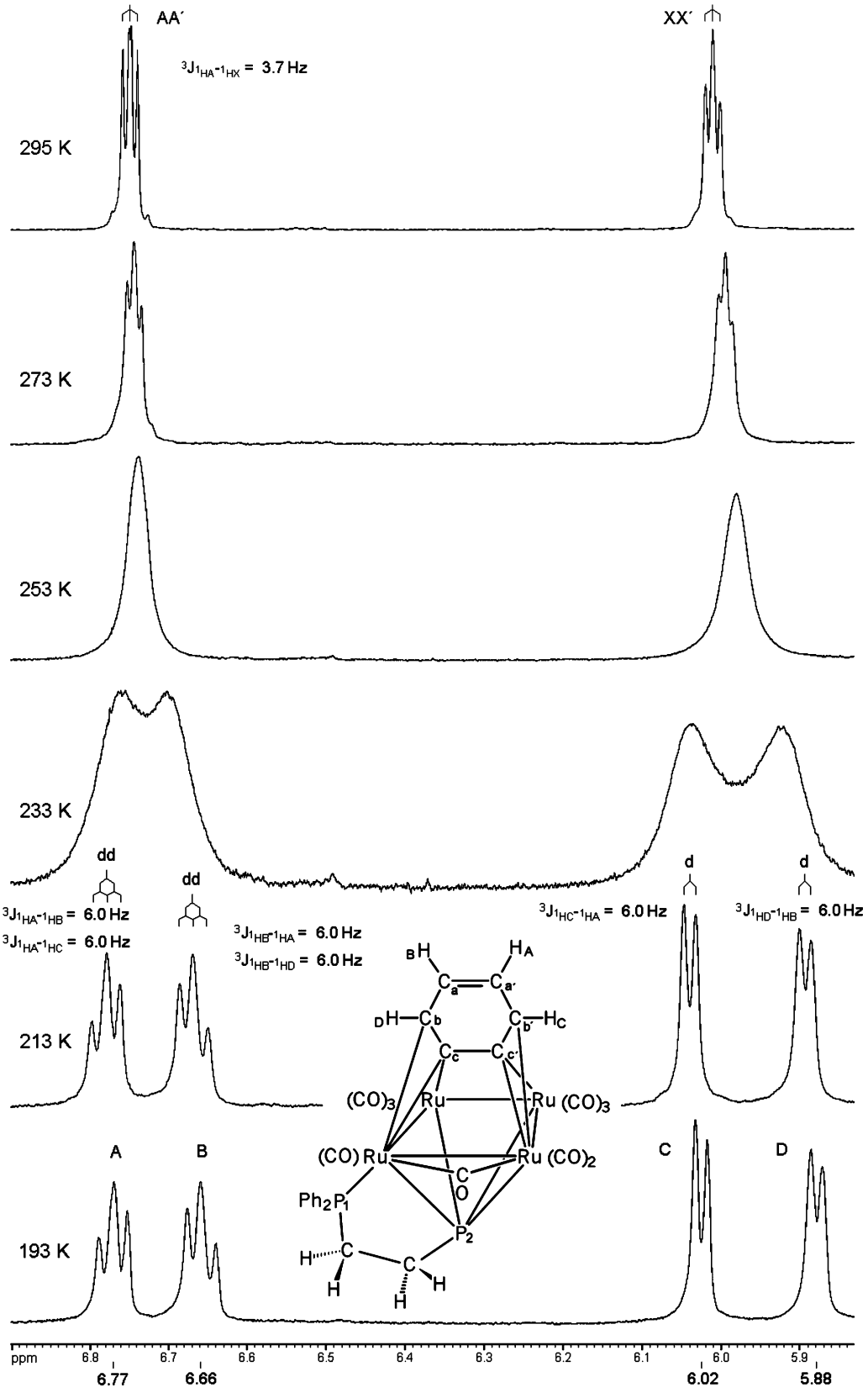

Fig. 2. ^{1}H-NMR spectrum of compound **2** at different temperatures, in the region of the benzyne ring (in CD_2Cl_2).

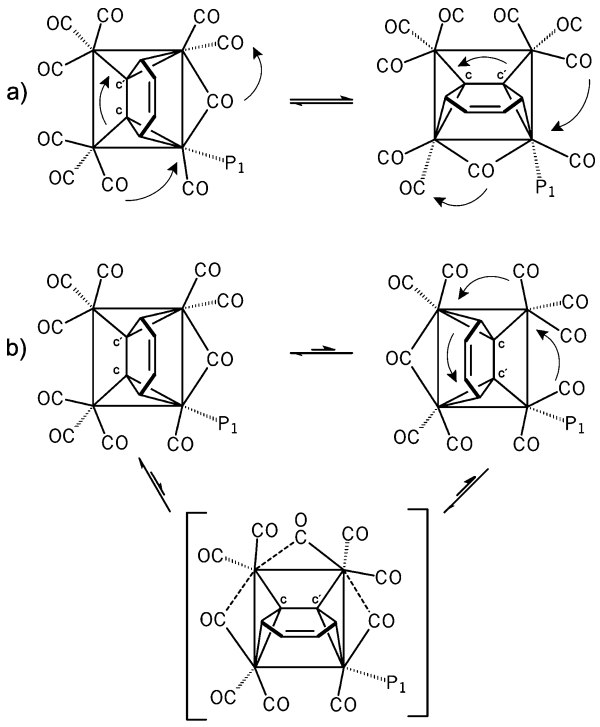

Scheme 3. (a) Proposed mechanism for benzyne rotation in compound **2**. (b) Proposed mechanism for CO migration.

has the structure stablished by the X-ray method. The consideration of Scheme 3a reveals that the fast reversible process 1, gives already the averaging signals of the benzyne ring because both states in this process are enantiomeric. Add also that such an enantiomerization correlates well with the above behaviour of the diasterotopic protons in the CH_2–CH_2 bridge. However, process 1 does not lead to the complete averaging of the CO groups and hence acoording to Scheme 3a they should migrate slower. Unfortunately for objective reasons it was not possible to analyze quantitatively the CO migration by a correct CO line-shape analysis. Nevertheless the $^{13}C\{^1H\}$-NMR spectrum of **2**, recorded at 253 K, in the CO region shows clearly one (averaged) broadened resonance with $\Delta\nu$ of 226 Hz while the broadened lines, for example, C(a) and C(a′) are observed separately with the chemical shift differences of 290 Hz. These lines provide to calculate the rate of the benzyne migration as 360 Hz. A maximal chemical shift difference for the CO signals can be measured as 820 Hz at 193 K. This value and the above line width of the averaged signal ($\Delta\nu = 226$ Hz) leads to the migration rate estimated as 600–700 Hz. These data contradict Scheme 3a and the mechanism proposed by Knox et al. [4] where the ring migration controls kinetically the CO movement. In the absence of good evidences and remaining the reasonable idea about the above kinetic control, we can propose additional (to that shown in Scheme 3a) benzyne movement, shown in the Scheme 3b, which leads to the CO migration but not to the averaging the benzyne environment. This process implies the movement of two of the terminal CO to semibridging positions and the initial CO bridging also changes to a semi bridge position as shown in the proposed intermediary in Scheme 3b to give the preferred structure at the left of the Scheme. The population of the structure at the right side could be

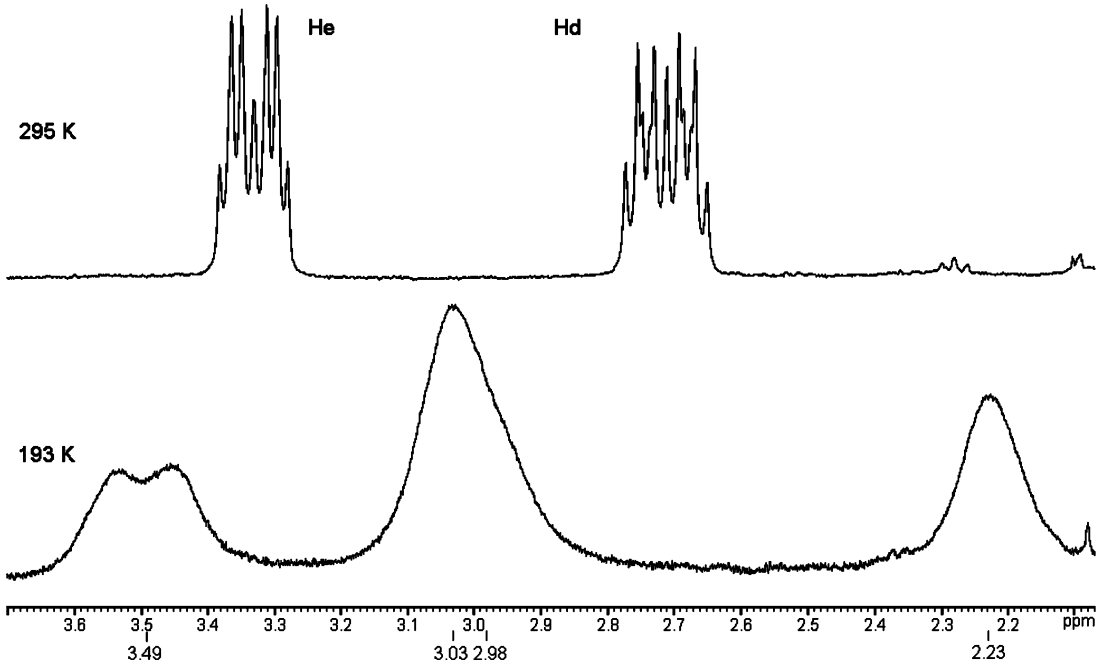

Fig. 3. ^{1}H-NMR spectrum of compound **2**, in the methylene region at 295 and 193 K (in CD_2Cl_2).

small at low temperature although we have no reasonable explanation for this.

Compound **3**, was also heated to reflux in toluene. After 2 h almost all of the starting material was still present in the solution and only traces of three other unidentified products. This, together with the analysis of the products obtained from the pyrolysis of **1**, suggests the higher thermal stability of compound **3**. Aromatic C–F bonds have been reported to have dissociation energies between 110 and 125 kcal mol^{-1} while C–H bonds are sligthly weaker with values between 100 and 112 kcal mol^{-1} [13]. This small difference makes it difficult to understand the higher stability of compound **3**. Selective C–F bond activation (over C–H activation) has been observed to occur in certain metal systems, but the opposite is observed in some other cases [14]. It is important to point out that we could not find examples of Ru carbonyl clusters containing M–F bonds; so perhaps the formation of this bond is not a favoured step in the process of oxidative addition of the ring.

3. Conclusions

The thermolysis reaction of $[Ru_3(CO)_{10}(dppe)]$ leads a similar product to described in the thermal reaction of $[Ru_3(CO)_{11}PPh_3]$, with formation of benzyne and μ_4-P groups, although the P–CH_2–CH_2–P unit remains. Variable temperature NMR studies of **2**, show this to have three types of movement which involve benzyne rotation, CO migration and a twisting movement of the CH_2–CH_2 chain. Thermolysis of $[Ru_3(CO)_{10}(dfppe)]$ carried out under the same conditions showed almost no reaction. Perhaps the initial orthometallation reaction is not favourable when C_6F_5 rings are present.

4. Experimental

4.1. General procedures and materials

All reactions and manipulations were carried out under nitrogen atmosphere. $[Ru_3(CO)_{12}]$, bis(dipentafluorophenylphosphino)ethane and bis(diphenylphosphino)ethane, were bought from Strem or Aldrich and were used as received. Solvents were purified by standard methods. Infrared spectra were recorded in solution in a Perkin–Elmer 2000 spectrometer. NMR spectra were obtained using a JEOL GSX-270, a JEOL Eclipse 400 or a Bruker Avance™ DPX 300 spectrometer, with ^1H and ^{13}C spectra relative to $SiMe_4$, ^{31}P-NMR relative to 85% aq. H_3PO_4. All NMR spectra were obtained in $CDCl_3$ unless otherwise stated. In the cases where multinuclei systems were present, two-dimensions spectra and selective homo- and heteronuclear irradiation experiments were performed in order to assign unequivocally the different signals. Elemental analysis were carried out in the University of Oviedo, in Spain. The mass spectrum was obtained at the National Autonomous University of México, in México City.

4.2. Thermal reaction of $[Ru_3(CO)_{10}L]$ (L = dppe or dfppe)

The phosphine substituted derivative **1** or **3** (50 mg) was dissolved in 30 ml of $C_6H_5CH_3$ and heated to refluxing temperature for 2 h. In the case of the dfppe derivative, most of the starting material was recovered unchanged, while in the dppe complex, four fractions were obtained by TLC using $CHCl_3$–C_6H_{14} 8:2. The fourth red fraction was identified as $[Ru_4(CO)_9(\mu\text{-}CO)\{\mu_4\text{–}\eta^2\text{-}PCH_2CH_2P(C_6H_5)_2\}(\mu_4\text{–}\eta^4\text{-}C_6H_4)]$ (**2**) (15.8 mg, 41%). Microanalysis: Calc.: C, 35.88; H, 1.81; Expt. C, 36.52; H, 2.09%. FABMS: 1005 $[M^+]$. IR ($CHCl_3$) : νCO) 2070(m), 2034(s), 2014(vs), 1978(m,br), 1955(w,br), 1890(w) cm^{-1}.

5. Crystallography

Crystals of **2** were grown from CH_2Cl_2 solution. Details of the data collection and structure refinement

Table 3
Data collections parameters and structure refinement details for **2**

	2
Empirical formula	$C_{30}H_{18}O_{10}P_2Ru_4$
Molecular weight	1004.66
Temperature (K)	220
λ (Mo–K_α) (Å)	0.71073
Crystal system	Triclinic
Space group	$P\bar{1}$
Unit cell dimensions	
a (Å)	10.5236(10)
b (Å)	11.1654(10)
c (Å)	15.2902(10)
α (°)	70.34(2)
β (°)	85.73(2)
γ (°)	71.02(2)
V (Å^3)	1598.6(2)
Z	2
ρ_{calc} (mg m^{-3})	2.087
μ(Mo–K_α) (Å)	2.009
F(000)	968
Scan type	$\omega/2\theta$
2θ Range (°)	4.78–52.58
Index ranges	
(h_{min}/h_{max}, k_{min}/k_{max}, l_{min}/l_{max})	−13/13, −12/13, 0/19
Reflections collected	6277
Independent reflections	6277 (R_{int} = 0.0200)
Observed reflections	3921 ($F > 4\sigma(F)$)
Final R indices [$F > 4\sigma(F)$]	R_1 = 0.0578, wR_2 = 0.1718 [a]
R indices (all data)	R_1 = 0.1159, wR_2 = 0.1950 [a]
Goodness-of-fit on F^2	0.967

[a] $w^{-1} = \sigma_2 F_o^2 + (0.1275P)^2 + 0.0000P$, where $P = (F_o^2 + 2F_c^2)/3$.

procedures are summarized in Table 3. Data was collected in an Enraf–Nonius CAD4 diffractometer. The samples were mounted in capillary tubes. The structure was solved by direct methods (SHELXS-97). [15] All non-hydrogen atoms were found in Fourier maps and refined anisotropically. Hydrogen atoms from phenyl groups were fixed in idealized positions. Absorption corrections were carried out by empirical methods. All calculations were carried out in PC computers.

6. Supplementary material

Crystallographic data for the structural analysis have been deposited with the Cambridge Crystallographic Data Center, CCDC no. 145731 for compound **2**. Copies of this information may be obtained free of charge from The director, CCDC, 12 Union Road, Cambridge CB2 1EZ, UK (fax.: (int code)+44-1223-336033; e-mail: deposit@ccdc.cam.ac.uk or www: http://www.ccdc.cam.ac.uk).

Acknowledgements

G.S.C. and F.J.Z. wish to thank Conacyt for a grant. V.B. also thanks Conacyt for the award of a *Cátedra Patrimonial de Excelencia* (Num. 990444-EX). We also wish to thank V.M. González and M.A. Leyva for their technical assistance. Dr J. Cabeza from the University of Oviedo in Spain is gratefully acknowledged for his help.

References

[1] D.F. Shriver, H.D. Kaesz, R.D. Adams, The Chemistry of Metal Cluster Complexes, VCH, 1990, p. 121.
[2] J.M. Fernandez, B.F.G. Johnson, J. Lewis, P.R. Raithby, J. Chem. Soc. Dalton Trans. (1981) 2250.
[3] R.D. Adams, B. Captain, W. Fu, M.D. Smith, J. Organomet. Chem. 651 (2002) 124.
[4] S.A.R. Knox, B.R. Lloyd, D.A.V. Morton, S.M. Nicholls, A.G. Orpen, J.M. Viñas, M. Weber, G.K. Williams, J. Organomet. Chem. 394 (1990) 385.
[5] N. Lugan, J.J. Bonnet, J.A. Ibers, J. Am. Chem. Soc. 107 (1985) 4485.
[6] M.I. Bruce, N.N. Zaitseva, B.W. Skelton, A.H. White, J. Organomet. Chem. 515 (1996) 143.
[7] G. Sánchez-Cabrera, F.J. Zuno-Cruz, M.J. Rosales-Hoz, A. Vela-Amieva, J. Chem. Soc. Dalton Trans. Submitted for publication.
[8] M.I. Bruce, G. Shaw, F.G.A. Stone, J. Chem. Soc. Dalton Trans. (1972) 2094.
[9] A.J. Deeming, R.E. Kember, M. Underhill, J. Chem. Soc. Dalton Trans. (1973) 2589.
[10] A.J. Deeming, I.P. Rothwell, M.B. Hursthouse, J.D.J. Backer-Dirks, J. Chem. Soc. Dalton Trans. (1981) 1879.
[11] S. Field, R.J. Haines, D.N. Smit, J. Chem. Soc. Dalton Trans. (1988) 1315.
[12] G. Hägele, R. Spiske, H.W. Höffken, T. Lenzen, U. Weber, Z. Gpudetsidis, Phosphorus Sulfur Silicon 77 (1993) 282.
[13] (a) D. Cox, G. Pilcher, Thermochemistry of Organic and Organometallic Compounds, Academic Press, New York, 1970; (b) S.W. Benson, Thermochemical Kinetics, John Wiley & Sons, 1968.
[14] L. Cronin, C.L. Higgets, R. Karch, R.N. Perutz, Organometallics 16 (1997) 4920.
[15] G.M. Sheldrick, SHELX-97, A Program of Crystal Structure Refinement, Institut fur Anorganische Chemie der Universität, Tammanstrastrasse 4, D-3400 Göttingen, Germany, 1997, Release 97-2.